



Relationships among the chemical, mechanical and geometrical properties of basalt fibers

Calvin Ralph , Patrick Lemoine, John Summerscales , Edward Archer and Alistair McIlhagger

Textile Research Journal
0(00) 1–11

© The Author(s) 2018

Article reuse guidelines:

sagepub.com/journals-permissions

DOI: 10.1177/0040517518805376

journals.sagepub.com/home/trj



Abstract

We investigated the chemical, mechanical and geometrical properties of basalt fibers from three different commercial manufacturers and compared the results with those from an industry standard glass fiber. The chemical composition of the fibers was investigated by X-ray fluorescence spectrometry, which showed that basalt and glass fibers have a similar elemental composition, with the main difference being variations in the concentrations of primary elements. A significant correlation between the ceramic content of basalt and its tensile properties was demonstrated, with a primary dependence on the Al_2O_3 content. Single fiber tensile tests at various lengths and two-way ANOVA revealed that the tensile strength and modulus were highly dependent on fiber length, with a minor dependence on the manufacturer. The results showed that basalt has a higher tensile strength, but a comparable modulus, to E-Glass. Considerable improvements in the quality of manufacturing basalt fibers over a three-year period were demonstrated through geometrical analysis, showing a reduction in the standard deviation of the fiber diameter from 1.33 to 0.61, comparable with that of glass fibers at 0.67. Testing of single basalt fibers with diameters of 13 and 17 μm indicated that the tensile strength and modulus were independent of diameter after an improvement in the consistency of fiber diameter, in line with that of glass fibers.

Keywords

basalt fibers, chemical properties, mechanical properties, physical properties

Environmental issues, such as the waste disposal and recyclability of composites, are becoming increasingly important to both industry and governments and have led to the promotion of natural fibers as reinforcements in polymer composites.^{1–3} Fibers typically used as reinforcements in polymers are glass or carbon fibers due to their good mechanical properties, especially their strength; however, they are not environmentally friendly.^{4,5} Natural fibers, including plant fibers such as kenaf and flax, have poor mechanical properties and are prone to thermal degradation,^{6,7} making them uncompetitive with glass and carbon fibers. This has led to a focus on basalt fibers.

Continuous basalt fibers have a simple manufacturing process that does not require any additives.⁸ Basalt fibers are produced by melting basalt rock at temperatures between 1350 and 1700 °C and then pulling the molten material downwards through a

platinum–rhodium die (bushing) using the spinneret method.⁹ The melting of basalt rock is conducted in two stages: it is first fused in the initial furnace and then transferred to the primary furnace, which controls the temperature of the melt and feeds the bushings.¹⁰ The fibers for processing are primarily heated by overhead gas heaters. The dark color of basalt means that material close to the surface of the melt absorbs infra-red energy from the gas burners, making it difficult to obtain a homogeneous melt. There are two methods to

University of Ulster at Jordanstown, UK

Corresponding author:

Calvin Ralph, University of Ulster at Jordanstown, Shore Road, Newtownabbey BT37 0QB, UK.

Email: ralph-c@ulster.ac.uk

overcome this: holding the basalt melt in the heating stage for longer or, more commonly, using immersed electrodes to electrically heat the melt.^{10,11}

The chemical composition of basalt varies depending on the geographical location and conditions of formation of the source rock. Basalt consists primarily of silicon, aluminum, calcium and iron oxides, similar to glass fibers.^{12–14} Fibers produced from basalt consist of the minerals olivine, plagioclase, pyroxene and clinopyroxene.¹⁵ Basalt is classified according its SiO₂ content, where alkali basalts contain up to 42% SiO₂, mildly acidic basalts contain 43–46% SiO₂ and acidic basalts contain >46% SiO₂. To manufacture continuous basalt fibers, the basalt rock must fall within the acidic class (>46% SiO₂).¹⁶ Recent research¹⁷ has shown that the melting properties of basalt used in manufacturing fibers varies depending on the mineral class of the basalt rock. The melting process is a crucial stage in the production of continuous basalt fibers and the homogeneity of the melt can affect the quality, diameter and performance stability of the basalt fibers. The ability to produce basalt fibers with a consistent diameter is important if these fibers are to compete with glass fibers. Significant variations in fiber diameter will affect the fiber quality, the ability to model basalt composites, the fiber volume fraction and, potentially, the interfacial adhesion through increased or reduced surface area.^{18,19}

Basalt fibers have superior mechanical properties to plant fibers and comparable, or better, properties to glass fibers.^{3,18,20} The density of basalt is between 2.6 and 2.7 g/cm³, whereas the density of E-Glass is 2.5–2.6 g/cm³.²¹ Basalt fibers have excellent sound insulation, a thermal resistance higher than that of glass, good chemical resistance to both acidic and alkaline conditions (higher than E-Glass) and are biologically inert.^{12,22,23} The cost of basalt fibers (about £6.00/kg) is currently higher than that of E-Glass (about £1.50/kg), although lower than that of S-Glass (about £16.00/kg). E-Glass fiber manufacturing costs have economies of scale as an established reinforcement material, whereas basalt fiber production costs are compromised by early stage small-scale production. As basalt is the most common rock on Earth, there is an abundant supply available; however, because basalt fibers require a certain SiO₂ content, there are currently only about three dozen mines and quarries with certified rock suitable for fiber manufacture, with the majority in Ukraine and Russia.²⁴ The properties of basalt, together with its environmentally friendly nature,²⁵ mean that it has potential as a competitor or replacement for glass fiber and as a new fiber in various applications. Short and continuous basalt fibers have therefore been the focus of recent research with the aim of identifying their potential applications.^{12,21,26–34}

With the increased demand for basalt fibers, there has been an increase in the number of established manufacturers. Glass fibers have a relatively standard performance, whereas the performance and quality of basalt fibers from different sources or manufacturers has not yet been fully examined. It is therefore important to understand the variations in basalt fibers from different manufacturers, such as the chemical composition, consistency of diameter and mechanical properties. The aim of this work was to analyze these factors and to determine whether there are any variations or relationships between them.

Materials and methods

Materials

Several types of commercial basalt fiber were characterized and compared with commercially available glass fibers (Table 1). Each fiber was provided in the direct roving form with a general purpose size primarily suitable for use in epoxies. Companies A and C were chosen due to their long establishment and classification among the world leaders in basalt fiber manufacture, whereas Company B is a relatively new (5 years) and fast-emerging competitor within the market. E-Glass from Company D was selected because they are a well-established glass fiber manufacturer.

Methods

X-ray fluorescence spectrometry. The chemical composition of the fibers was determined by X-ray fluorescence (XRF) spectrometry. The fibers were initially placed in a muffle furnace at $T = 650\text{ }^{\circ}\text{C}$ for 30 minutes to remove any sizing present on the fibers. Pyrolysis is commonly used to remove sizing and the temperatures and time used in this work were higher than those reported to be required to remove all organic sizing.^{35–37} After cooling, the desized fibers were milled for 2 minutes at

Table 1. Basic data for the investigated fibers

Designation	Fiber type	Manufacturer	Nominal diameter (μm)	Linear density (Tex)
BF1	Basalt	Basaltex	13	150
BF2	Basalt	Mafic	13	300
BF3	Basalt	GBF	13	400
BF4	Basalt	Basaltex	17	600
BF5	Basalt	Mafic	17	500
Glass fibers	Glass	PPG	14	300

520 rpm in a Retsch PM100 planetary ball-mill to achieve a consistent powder. The powder fiber samples were mixed with CEREOX Licowax (Fluxana, BM-0002) at a ratio of 4:1 to bind the powder and then pressed (Retsch PP25) to produce pellets for XRF analysis. CEREOX was used as a binding agent because it is clean and stable under X-rays and is designed specifically for XRF because it does not influence the results. XRF spectrometry was performed using a Thermo Scientific Niton FXL FM-XRF analyzer. Each sample was tested in three spots with a testing time of 150 s per spot.

Analysis of fiber diameters. Scanning electron microscopy (SEM) with a JEOL JSM-6010 microscope was used to determine the actual fiber diameter of the basalt and glass samples. Fibers were coated with gold to improve the image quality and accuracy. A set of 100 measurements was recorded from 15 mm samples taken at 1 m intervals along the roving length to give a total of 300 measurements per fiber type. Fiber sizing was not removed prior to the measurements because the calculated sizing thickness was <16 nm and therefore negligible. SEM was used instead of standard optical microscopy due to its increased image quality.

Mechanical testing. Single fiber tensile tests were performed according to ASTM D3379 using an Instron 5564 instrument with a 200 N load cell. As-received fibers were separated and bonded to cardboard templates, clamped in the grips of the test machine and the template was carefully cut before the start of the test. A minimum of 10 tests was performed for each sample at a constant crosshead rate of 1 mm/min for 25, 50 and 100 mm gage lengths. As it was not possible to use an extensometer or strain gage due to the small diameter of the fragile fibers, the recorded load versus displacement results were used in conjunction with the compliance method stated in ASTM D3379.

The indicated compliance was calculated using equation (1).

$$C_a = (I/P)x(H/S) \tag{1}$$

where I is the total extension for straight line section of the load–time curve extrapolated across the full chart scale, P is the full scale force, H is the crosshead speed and S is the chart speed. The true compliance is then calculated as:

$$C = C_a - C_s \tag{2}$$

where C_s is the system compliance. Young’s modulus was calculated as a corrected value using the following equation:

$$E = L/CA \tag{3}$$

where L is the specimen gage length and A is the average filament area.

Results and discussion

The chemical composition of the studied fibers is given in Table 2. The primary compound found within both the basalt and E-Glass fibers is SiO₂. The basalt fibers have a relatively consistent SiO₂ content of 48.82–49.69 mass per cent (mass%) across different manufacturers, consistent with the requirement to spin continuous basalt fibers. The glass fibers had a higher SiO₂ content of > 53 mass%, in agreement with previous studies and specifications.^{9,12,38,39} The basalt fibers contained five essential elemental components (SiO₂, Al₂O₃, CaO, MgO and Fe₂O₃). Similarly, the glass fibers were mainly formed from five primary groups (SiO₂, Al₂O₃, CaO, MgO and B₂O₃). Boron could not be determined with the equipment used in this work, but it is known that glass fibers contain 0.4–5 mass%

Table 2. Chemical composition of basalt and glass fibers

Element	Oxide	BF1		BF2		BF3		Glass fibers	
		Element (mass%)	Oxide (mass%)	Element (mass%)	Oxide (mass%)	Element (mass%)	Oxide (mass%)	Element (mass%)	Oxide (mass%)
Si	SiO ₂	22.52	48.82	23.22	49.69	23.26	49.58	24.78	53.02
Al	Al ₂ O ₃	6.79	12.83	7.12	13.45	6.11	11.54	5.91	11.16
Ca	CaO	4.50	6.02	4.51	6.03	3.62	4.85	12.53	16.77
Fe	Fe ₂ O ₃	5.18	7.41	5.25	7.51	4.87	6.96	0.17	0.24
Mg	MgO	2.45	4.06	2.03	3.36	3.08	5.10	1.82	3.02
Ti	TiO ₂	0.56	1.18	0.58	1.21	0.43	0.90	0.05	0.10
K and Na	K ₂ O+Na ₂ O	1.12	2.44	1.20	2.50	1.67	2.13	0.27	0.36

boron, with the exception of some new boron-free glass fibers, but boron is not present in basalt.^{9,38,40,41} The glass fibers shared further oxides with basalt fibers, such as TiO₂, K₂O, Na₂O and Fe₂O₃, but in much lower quantities (<1 mass%). These results highlight the chemical differences between glass and basalt fibers, with the higher content of Fe₂O₃ contributing to the increased temperature resistance and darker color of basalt fibers. With the exception of a small variation in the SiO₂ and Al₂O₃ contents (about 1 mass%), samples BF1 and BF2 had a similar chemical composition. Sample BF3 had a similar SiO₂ content to BF1 and BF2, but varied consistently by 1–2 mass% for all other elements. A higher CaO content reduces the melting temperature of basalt and leads to easier homogenization of the melt, which known to aid fiber production.⁴² Samples BF1 and BF2 had a similar CaO content, whereas the CaO in sample BF3 was about 1.25 mass% lower, which could lead to an inhomogeneous melt unless adjustments are made to the furnace temperature.

Fibers from sample BF2 were chosen for further investigation to determine the consistency of fiber manufacture over time. Table 3 gives details of the fibers tested. The batches of fibers were manufactured about one year apart. The average measured diameter did not vary significantly between years, but a clear change in the standard deviation is evident, with an improvement from 1.33 to 0.61. This deviation clearly shows considerable improvements in the consistency of fiber manufacture. The fiber diameter is related to

parameters such as the velocity of the molten material, the haul-off rate and the internal diameter of the bushing.⁴³ It is believed that improvements in the melt homogeneity result in better control of the diameter of basalt fibers, as seen with glass fibers.⁴⁴

The improved results for sample BF2 were compared with the diameters of fibers from other manufacturers (Table 4). In addition to fibers tested in this work, the results were compared with previous studies on Technobasalt and D.S.E Group fibers (designated samples BF6 and BF7, respectively).⁴⁵ The nominal diameter stated by the manufacturers of basalt fibers was 13 μm across all samples. Glass fibers were measured as 13.87 μm compared with the stated diameter of 14 μm, with a low standard deviation of 0.67. The diameter of basalt fibers needs to be consistent if they are to be competitive with glass fibers and to assist in the prediction and modeling of basalt composites. Figure 1 shows the distribution of fiber diameters each test fiber.

Fiber from one of the leading basalt manufacturers (sample BF1) was on average 1.16 μm larger than the specified diameter and had a higher standard deviation of 1.2. Although samples BF3 was close to its stated diameter, the standard deviation was more than double that of glass fibers. Sample BF6 fibers were > 1 μm larger than specified, with a very high standard deviation of 2.9, suggesting poor consistency in fiber manufacture. These results highlight the current gap between glass and basalt fibers in terms of fiber manufacture and quality. However, the improved fiber of sample BF2

Table 3. Results of measurements of fiber diameter for sample BF2

Manufacturer	Date of manufacture	Stated diameter (μm)	Measured diameter (μm)	Standard deviation
Mafic	February 2014	13	13.39	1.33
	April 2015	13	13.43	1.10
	August 2016	13	13.31	0.61

Table 4. Results of measurements of fiber diameters

Sample	Stated diameter (μm)	Average diameter (μm)	Standard deviation	Coefficient of variation (%)
BF1	13	14.16	1.20	8.46
BF2	13	13.31	0.61	4.61
BF3	13	12.61	1.38	10.97
BF6 (Ref. ⁴⁵)	13	14.1	2.9	4.76
BF7 (Ref. ⁴⁵)	13	12.70	1.50	4.00
Glass fibers	14	13.87	0.67	4.84

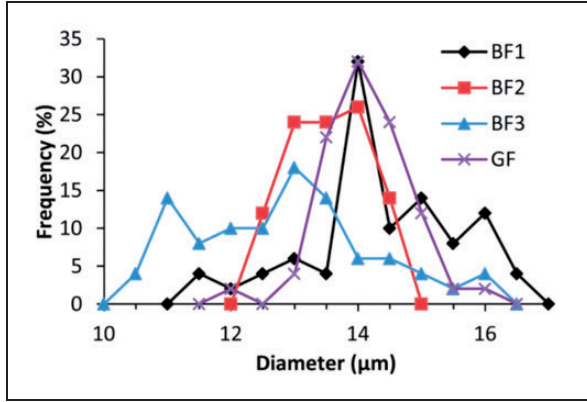


Figure 1. Distribution of the diameters of basalt and glass fiber samples.

showed significant improvements, with a diameter close to the stated value and, more importantly, a standard deviation of 0.61, lower than that of the glass samples. It is clear there have been some significant improvements in the manufacture and quality of basalt fibers in recent years. The larger diameter fibers of samples BF4 and BF5 had a high consistency in diameter with standard deviations of 0.83 and 0.69, respectively, although this is probably a result of the easier manufacturer of larger fibers.

The tensile strength and tensile modulus of all the 13 μm fibers are presented in Figure 2(a) and Figure 2(b), respectively. Initial observations of the tensile strength indicated that the fiber strength decreased as the fiber length increased for all fibers. This behavior is widely associated with an increase in the flaw population due to the longer fiber length and has been observed in both carbon and glass fibers.^{46,47}

There are two variables within these samples that may influence the mechanical properties: the fiber type/manufacturer and the fiber length. Two-way ANOVA was performed to determine the dependence of the tensile strength and modulus of the filaments on these two factors.⁴⁸ The prerequisite of ANOVA to determine the equality of variances was determined by the Levene test.⁴⁹ The test statistic W was calculated by:

$$W = \frac{(N - k) \sum_{i=1}^k N_i (\bar{Z}_i - \bar{Z})^2}{(k - 1) \sum_{i=1}^k \sum_{j=1}^{N_i} (Z_{ij} - \bar{Z}_i)^2} \quad (4)$$

where k is the number of different groups, N is the total number of measurements, $Z_{ij} = |Y_{ij} - \bar{Y}_i|$ where \bar{Y}_i is the mean of the i th group and Y_{ij} is the value of the measured variable for the j th case of the i th group, \bar{Z} is the mean of all Z_{ij} and \bar{Z}_i is the mean of the Z_{ij} for the i th group. The resulting P values for the tensile strength and tensile modulus were 0.23 and 0.49, which are significantly higher than the significance level ($\alpha = 0.05$).

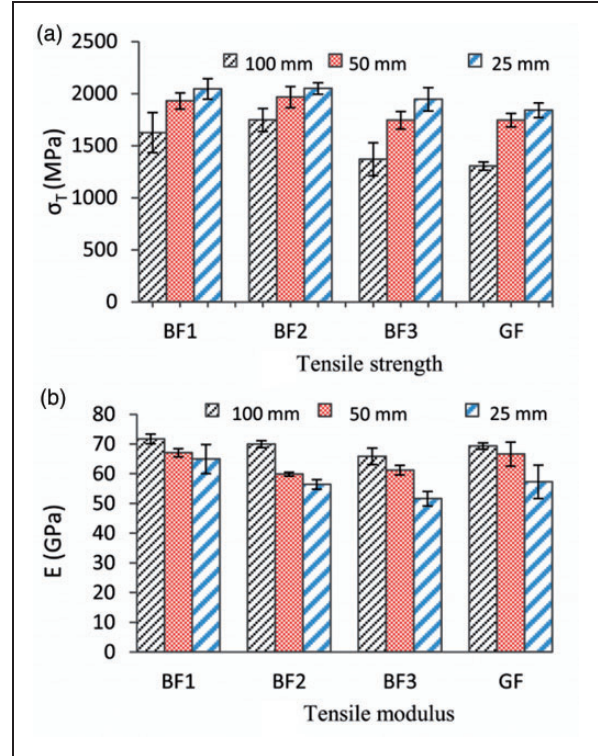


Figure 2. Tensile properties of 13 μm basalt and glass fibers.

Therefore the null hypothesis theory of standard variations can be accepted. ANOVA was then performed with the fiber type being Factor A and fiber length being Factor B. The calculated P values from ANOVA were used as results considering a significance level of $\alpha = 0.05$. The null hypothesis of equal means is accepted when $P > \alpha$ and hence rejected when $P < \alpha$.

Table 5 gives the results for the results of the two-way ANOVA for tensile strength and tensile modulus. The reported F value is the variation between the sample means/variation within the samples and is used for determining the P value. For tensile strength, the very low P value relating to the fiber length shows that variations in gage length are relevant at the 5% significance level, indicating a strong dependence of the strength on gage length. Low P values for Factor A also indicate a dependence of fiber strength on the fiber type/manufacturer. Previous studies have confirmed the strong dependence of basalt fiber strength on gage length,¹⁵ but indicated that there was no dependence on fiber type. When the lower values of sample BF3 were removed from the ANOVA analysis, the corresponding P value for fiber type increased to 0.5, which is in agreement with previous findings and highlights the poor mechanical performance of sample BF3 fibers. However, as sample BF3 is a commercially available fiber, it is important to include it in the

Table 5. Two-way ANOVA results for tensile properties of basalt fibers

Sample	Degrees of freedom	Tensile strength		Tensile modulus	
		F	P	F	P
Factor A (fiber type)	2	8.48	0.0364	9.46	0.0305
Factor B (fiber length)	2	28.28	0.0044	16.38	0.0118
Interaction	4	18.38	0.0077	12.92	0.0147

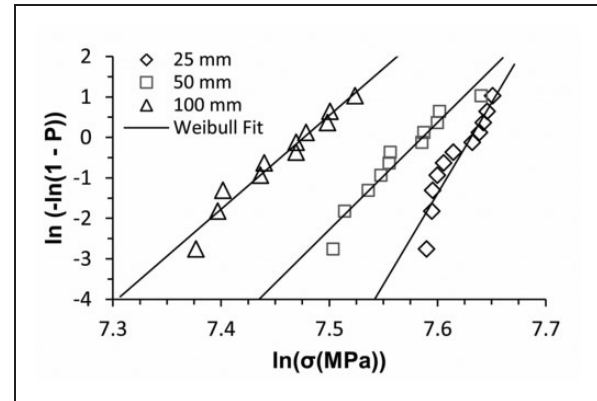
analysis and hence it can be suggested that there is a dependence of tensile strength on fiber type.

A similar trend for tensile modulus can be seen from ANOVA results. The low P values for both Factor A and Factor B show that the elastic modulus depends on both fiber type and fiber length. It has previously been suggested¹⁵ that the modulus did not depend on fiber length. This change may be explained by the gage lengths used during testing, which previously focused on 10–40 mm. When the values for the 100 mm gage length were removed from the ANOVA analysis, the corresponding P value for fiber length increased to 0.16, indicating that the tensile modulus across different fiber lengths was not significantly different. However, comparable testing performed on E-Glass fibers⁴³ with lengths of 5–80 mm showed that tensile modulus increased as the fiber length increased, in agreement with the results found for longer basalt fibers. This increase, despite the modulus correction, can be attributed to the dependency of the test equipment on the sample gage length. This dependency is manifested as a contribution to elastic deformation from the testing equipment and is in agreement with the work of Pardini and Manhani,⁴⁷ who reported an increase in modulus with gage length for both glass and carbon fibers with the ASTM correction and rigidity methods. Comparisons between glass and basalt fibers show that basalt is characterized by a higher tensile strength and a comparable elastic modulus to that of glass. It is noted that the mechanical properties are lower than the values stated in the technical data sheet.

The tensile data was further analyzed by applying Weibull statistics. Data for each fiber and each gage length were sorted in ascending order. From this, the corresponding value of the cumulative failure probability, P_F , was determined using the median rank estimator.⁵⁰

$$P_F = \frac{i - 0.3}{N + 0.4} \quad (5)$$

where i is the i th term of total number of tests N . The Weibull parameters m (shape) and σ_o (scale) were determined for each fiber manufacturer and gage length

**Figure 3.** Weibull plot for sample BF2 fibers.

by fitting the data points with the two-parameter Weibull distribution in equation (6):

$$\ln[-\ln(1 - P_F)] = m \ln(\sigma) - m \ln(\sigma_o) \quad (6)$$

Figure 3 shows the Weibull plots obtained from equation (6) for sample BF2 fibers and Table 6 gives the parameters m and σ_o for all fibers and lengths. The lower values of m for sample BF3 suggest that the flaws are less evenly distributed throughout the fiber, resulting in a greater scatter in strength.^{47,50,51} Samples BF1 and BF2 have similar values, with the exception of 100 mm lengths, where the m value for BF1 is considerably lower than that for BF, indicating a less homogeneous material over longer lengths.

As the Weibull parameters were obtained at different gage lengths, it is possible to predict the tensile strength at lengths outside the experimental range.⁵² This can be achieved using equation (7), in particular at a cumulative probability failure $P_F = 0.5$.

$$\sigma = \sigma_o \left[\frac{1}{A_o L_f} \ln 2 \right]^{1/m} \quad (7)$$

where A_o is the cross-sectional area and L_f is the gage length of the fibers. The resulting plot obtained using the parameters from Table 6 are shown in Figure 4. The predictions from the Weibull statistics for samples BF1

Table 6. Weibull parameters for strength of 13 μm basalt fibers

Fiber	25 mm		50 mm		100 mm	
	σ_o (MPa)	m	σ_o (MPa)	m	σ_o (MPa)	m
BF1	2065	38.19	1942	31.63	1730	12.71
BF2	2066	42.52	1971	26.38	1765	25.69
BF3	1972	18.56	1775	32.18	1477	15.67

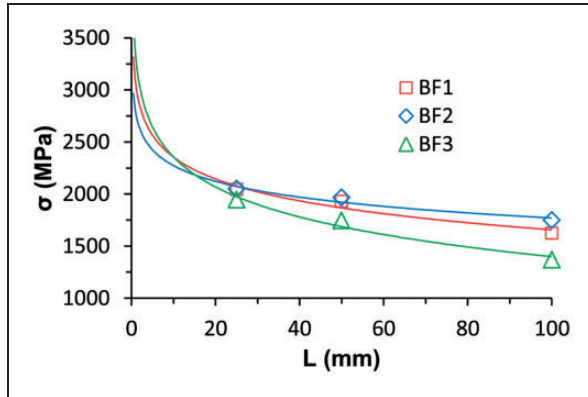


Figure 4. Tensile strength of 13 μm basalt fibers as a function of gage length.

and BF2 are very similar, with the exception of sample BF3, in agreement with the ANOVA results in Table 5, highlighting that there may be a difference between the strength of fibers from different manufacturers.

The mechanical properties of 17 μm fibers from Company B (BF5) and A (BF4) are shown in Figure 5. The 17 μm fibers show the same trend as the 13 μm fibers in that the tensile strength increases as the fiber length decreases and the tensile modulus increases as the length is increased.

The Weibull statistics were performed again for the 17 μm fibers. The m and σ_o Weibull parameters are shown in Table 7, whereas the prediction of strength at different lengths from equation (7) is presented in Figure 6.

Unlike the 13 μm fibers, there was a notable difference in strength between the 17 μm fibers in samples BF4 and BF5. Sample BF4 had a consistently lower m value at 25 and 50 mm gage lengths and was comparable at 100 mm, indicating that sample BF5 had better homogeneity.⁵⁰ The m value decreased at 100 mm length for both fibers, confirming that critical fiber flaws are more likely to be encountered at longer gage lengths. The difference in performance between samples BF4 and BF5 is shown in Figure 6.

It has widely been thought that the tensile strength and modulus of natural fiber increases as the fiber diameter decreases.^{53–56} This was shown by fibers

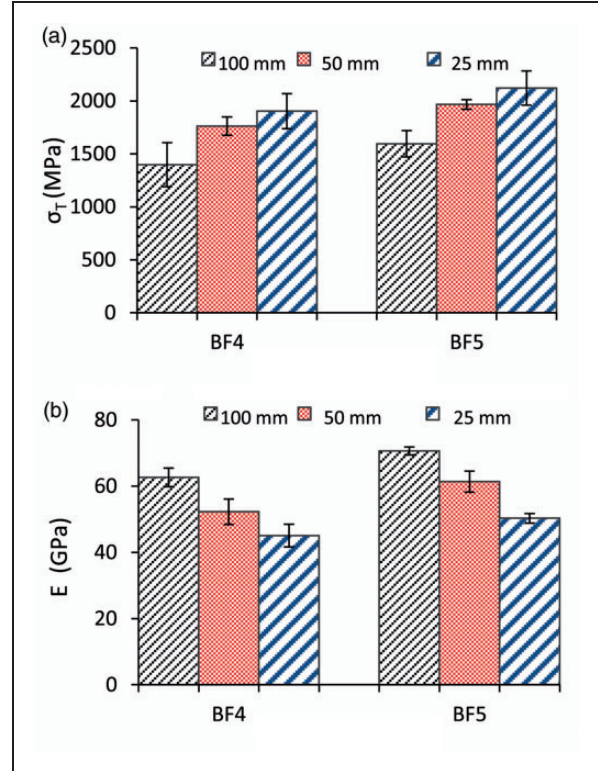


Figure 5. Tensile properties of 17 μm basalt and glass fibers.

Table 7. Weibull parameters for strength of 17 μm basalt fibers

Fiber	25 mm		50 mm		100 mm	
	σ_o (MPa)	m	σ_o (MPa)	m	σ_o (MPa)	m
BF4	1962	13.32	1797	28.6	1476	20.2
BF5	2210	20.2	2001	47.64	1634	15.66

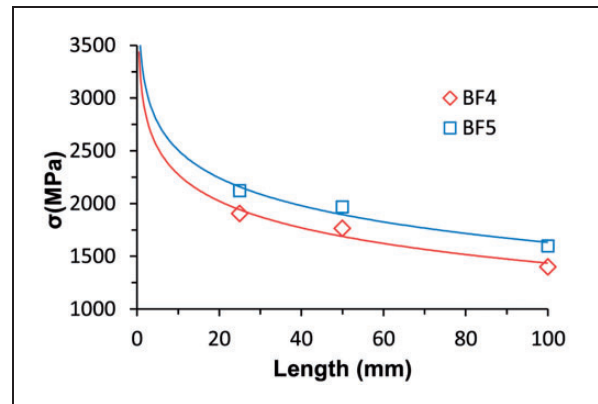


Figure 6. Tensile strength of 17 μm basalt fibers as a function of gage length.

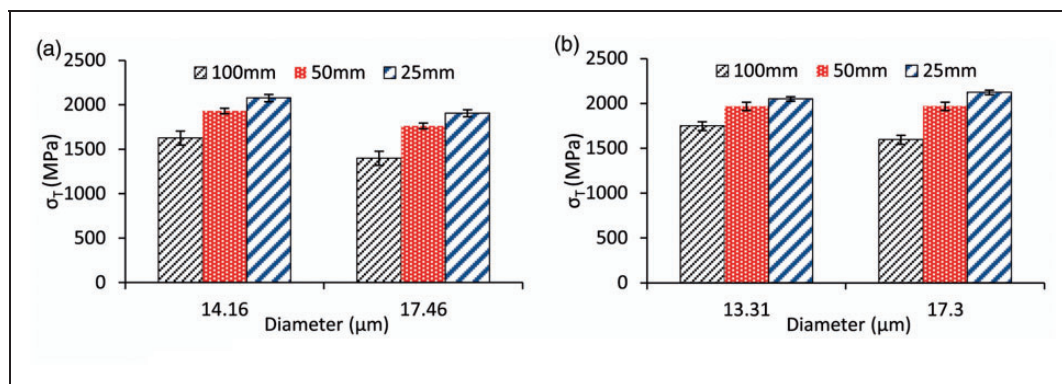


Figure 7. Diameter–tensile strength relationship for samples (a) BF4 and (b) BF5.

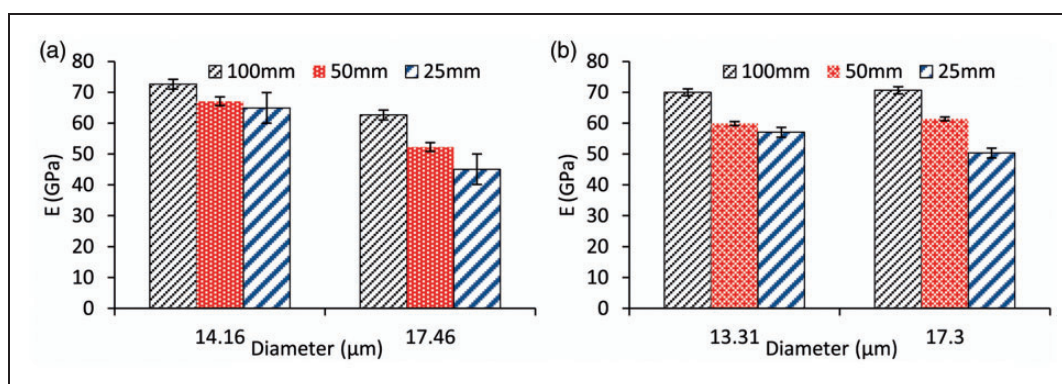


Figure 8. Diameter–tensile modulus relationship for samples (a) BF4 and (b) BF5.

from Company A, where there was a clear decrease in tensile strength and tensile modulus as the fiber diameter increased [Figure 7(a) and 8(a)]. By contrast, the tensile properties of glass do not depend on the fiber diameter as a result of improvements in the consistency of manufacture of glass fibers.⁵⁷ Comparisons of tensile strength and tensile modulus between the 13 and 17 μm basalt fibers from Company B (samples BF2 and BF5) can be seen in Figures 7(b) and 8(b).

The tensile strength is nearly constant for the two fiber diameters of samples BF2 and BF5, with the exception of the longer 100 mm lengths, where a slight reduction in strength is seen at larger diameters. The cause of this difference is unknown, although there are more likely to be critical fiber flaws in longer fiber lengths, which may be more prominent at larger diameters. The tensile modulus for sample BF5 showed little deviation, suggesting that tensile strength is independent of fiber diameter.

The independence of fiber strength and diameter for samples from Company B is in agreement with previous work.⁴⁵ Otto⁵⁷ showed that, when fibers of different diameters are formed under controlled, near-identical conditions, their break strengths are identical and hence

are reliant on the process of formation rather than the diameter. This applies to diameters >9 μm. With the demonstrated increase in the quality of basalt fibers from Company B, basalt fibers are shown to behave in a similar manner. These findings apply only to fibers on their own and not fibers embedded in a polymer matrix. Fibers tows consisting of fibers with a smaller diameter, but constant weight, have an increased surface area, which, in turn, generates more interaction and adhesion to the matrix and results in a higher mechanical performance.¹⁹ However, as the fibers begin with the same mechanical properties, it is thought that the effect of surface area may not be as large as for fibers that have a different performance at varying diameters.

The mechanical properties of basalt and glass fibers have been related to their chemical composition. Attempts have therefore been made to improve the mechanical properties of basalt fibers through the addition of extra elements during manufacturing, resulting in positive improvements.⁵⁸ A relationship between the ceramic-like content ($\text{SiO}_2 + \text{Al}_2\text{O}_3$), which is the primary composition of basalt, and the mechanical properties has been demonstrated; however, a correlation

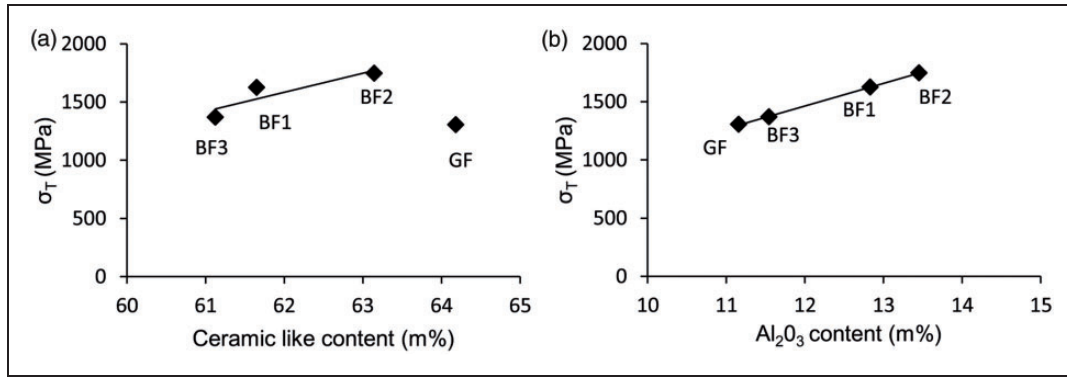


Figure 9. Chemical composition—tensile strength relationships.

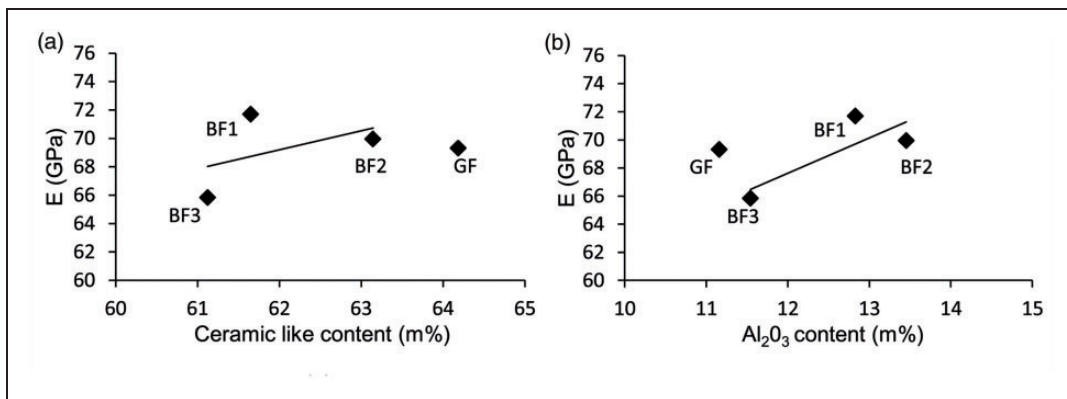


Figure 10. Chemical composition—tensile modulus relationships.

with the Al_2O_3 was not seen.⁴² Figure 9 shows the relationship between the tensile strength and the ceramic-like and Al_2O_3 contents.

Although glass fibers are shown on the same graph in Figure 9, they were not included in the correlation due to their different chemical composition. There is a clear correlation between tensile strength and the ceramic-like content (Figure 9(a)), but also a significant relationship with the Al_2O_3 content (Figure 9(b)). Two-way ANOVA was performed for tensile strength with the ceramic content as Factor A and the Al_2O_3 content as Factor B. The ceramic content generated a P value of 0.001, below the level of significance ($\alpha = 0.05$). The resulting P value for Al_2O_3 was considerably lower at 1.3523×10^{-7} , suggesting that the tensile strength is more dependent on the Al_2O_3 content. Comparisons with the tensile modulus (Figure 10) indicate that there is no significant correlation between the modulus and the ceramic-like or Al_2O_3 content. Similar comparisons of mechanical properties with other elements found within basalt fibers yielded no evident relationship, suggesting they have a low importance in directly determining the mechanical properties of fibers.

Conclusions

The chemical composition, fiber diameter and mechanical properties of different basalt fibers were investigated using XRF spectrometry, SEM and tensile testing. The main components of the basalt fibers were SiO_2 , Al_2O_3 , CaO , MgO and Fe_2O_3 , with small amounts of TiO_2 , K_2O and Na_2O . The glass fibers had similar chemical components/constituents to basalt, with the main difference in composition being higher levels of Fe_2O_3 in basalt. The chemical composition of basalt remained largely consistent between manufacturers, with only sample BF3 showing a variation in Al_2O_3 , CaO and MgO content. The diameter of the basalt fibers varied between manufacturers, with most showing a higher standard deviation than glass. Significant improvements in the distribution of fiber diameters was demonstrated for the first time, with sample BF2 being comparable with the glass fiber standard, suggesting advancements in the manufacturing quality of basalt fibers.

The mechanical properties of basalt fibers vary between manufacturers, although the properties of fibers from Company A and Company B were

comparable. The basalt fibers were characterized by a higher tensile strength than the E-Glass fibers and a similar tensile modulus. ANOVA was used to show the dependence of fiber strength on gage length, with shorter fiber lengths yielding a higher tensile strength and fiber lengths >50 mm yielding a higher tensile modulus.

For most of the commercial basalt fibers tested, the properties of the basalt fibers was dependent on the fiber diameter. Contrary to common belief, the strength and modulus of basalt fibers was independent of the fiber diameter for fibers from Company B, with fibers ranging from 13 to 17 μm diameter displaying comparable properties. A clear correlation between the mechanical properties and the chemical composition of basalt fibers was evident, with fibers showing a strong dependence on the ceramic-like content ($\text{SiO}_2 + \text{Al}_2\text{O}_3$), but primarily the Al_2O_3 content, confirmed by ANOVA. Basalt fiber technology has reached a point where adoption should no longer be constrained by product variability. The cost and performance of fibers currently lies between those for E-Glass and S2-Glass. The wider adoption of basalt fibers as reinforcement in composites will require mass production to meet the demand for fibers and should lead to their costs becoming competitive with the established E-Glass reinforcement.

Acknowledgements

The authors thank Ulster University, Northern Ireland Advanced Composites and Engineering Centre and Axis Composites for support and provision of testing equipment and Mafic Basalt for the provision of materials.

Declaration of conflicting interests


The authors declared no potential conflicts of interest with respect to the research, authorship, and/or publication of this article.

Funding

The authors disclosed receipt of the following financial support for the research, authorship, and/or publication of this article: This work was supported and funded by a Department for Employment and Learning CAST award Grant number B00527885.

ORCID iD

Calvin Ralph  <http://orcid.org/0000-0001-9307-820X>

John Summerscales  <http://orcid.org/0000-0002-3557-0404>

References

- Lopresto V, Leone C and De Iorio I. Mechanical characterisation of basalt fibre reinforced plastic. *Compos B Eng* 2011; 42: 717–723.
- Al-Oqla FM and Sapuan SM. Natural fiber reinforced polymer composites in industrial applications: Feasibility of date palm fibers for sustainable automotive industry. *J Clean Prod* 2014; 66: 347–354.
- Ku H, Wang H, Pattarachaiyakoo N, et al. A review on the tensile properties of natural fiber reinforced polymer composites. *Compos B Eng* 2011; 42: 856–873.
- Das S. Life cycle assessment of carbon fiber-reinforced polymer composites. *Int J Life Cycle Assess* 2011; 16: 268–282.
- PwC. *Sustainable Performance and Strategy. Life cycle assessment of CFGF-Continuous Filament Glass Fibre Products*. London: PriceWaterhouseCoopers, 2016.
- Arbelaiz A, Fernández B, Ramos JA, et al. Mechanical properties of short flax fibre bundle/polypropylene composites: Influence of matrix/fibre modification, fibre content, water uptake and recycling. *Compos Sci Technol* 2005; 65: 1582–1592.
- Gassan J and Bledzki A. Thermal degradation of flax and jute fibers. *J Appl Polym Sci* 2001; 82: 1417–1422.
- Bashatnik PI, Kabak AI and Yakovchuk YY. The effect of adhesion interaction on the mechanical properties of thermoplastic basalt plastics. *Mech Compose Mater* 2003; 39: 85–88.
- Militký J, Kovačič V and Rubnerová J. Influence of thermal treatment on tensile failure of basalt fibers. *Eng Fract Mech* 2002; 69: 1025–1033.
- Gur'ev V, Neproshin EI and Mostovoi GE. The effect of basalt fiber production technology on mechanical properties of fiber. *Glass Ceram* 2001; 58: 62–65.
- Fourné F. *Synthetic fibers*. Munich: Carl Hanser, 1999.
- Liu Q, Shaw MT and Parnas RS. Investigation of basalt fiber composite mechanical properties for applications in transportation. *Polym Compos* 2006; 27(1): 41–48.
- Czigány T. Discontinuous basalt fiber-reinforced hybrid polymer composites. In: Friedrich K (ed.) *Polymer composites: From nano to macro-scale*. Munich: Springer, 2005, pp.309–328.
- Czigány T. Trends in fiber reinforcements – the future belongs to basalt fiber. *Express Polym Lett*. 2007; 1: 59.
- Greco A, Maffezzoli A, Casciaro G, et al. Mechanical properties of basalt fibers and their adhesion to polypropylene matrices. *Compos B Eng* 2014; 67: 233–238.
- Militký J and Kovačič V. Ultimate mechanical properties of basalt filaments. *Textile Res J* 1996; 66: 225–229.
- Chen X, Zhang Y, Hui D, et al. Study of melting properties of basalt based on their mineral components. *Compos B Eng* 2017; 116: 53–60.
- Fiore V, Scalici T, Di Bella G, et al. A review on basalt fibre and its composites. *Compos B Eng* 2015; 74: 74–94.
- Dhand V, Mittal G, Rhee KY, et al. A short review on basalt fiber reinforced polymer composites. *Compos B Eng* 2015; 73: 166–180.
- Djafari Petroudy SR. 3 – Physical and mechanical properties of natural fibers. In: Fan M and Fu F (eds) *Advanced high strength natural fibre composites in construction*. Cambridge: Woodhead Publishing, 2017, pp.59–83.
- Czigány T. Special manufacturing and characteristics of basalt fiber reinforced hybrid polypropylene

- composites: Mechanical properties and acoustic emission study. *Compo Sci Technol* 2006; 66: 3210–3220.
22. Landucci G, Rossi F, Nicoletta C, et al. Design and testing of innovative materials for passive fire protection. *Fire Saf J* 2009; 44: 1103–1109.
 23. Wei B, Cao H and Song S. Environmental resistance and mechanical performance of basalt and glass fibers. *Mater Sci Eng A* 2010; 527: 4708–4715.
 24. Ross A. *Basalt fibers: Alternative to glass?* <https://www.compositesworld.com/articles/basalt-fibers-alternative-to-glass> (2006, accessed 21 April 2018).
 25. Jamshaid H and Mishra R. A green material from rock: Basalt fibre – a review. *J Textile Inst* 2016; 107: 932–937.
 26. Botev M, Betchev H, Bikiaris D, et al. Mechanical properties and viscoelastic behavior of basalt fiber-reinforced polypropylene. *J Appl Polym Sci* 1999; 74: 523–531.
 27. Bhat T, Chevali V, Liu X, et al. Fire structural resistance of basalt fibre composite. *Compos A Appl Sci Manuf* 2015; 71: 107–115.
 28. Ding L, Liu X, Wang X, et al. Mechanical properties of pultruded basalt fiber-reinforced polymer tube under axial tension and compression. *Construct Build Mater* 2018; 176: 629–637.
 29. Pawłowski D and Szumigala M. Flexural behaviour of full-scale basalt frp rc beams – experimental and numerical studies. *Procedia Eng* 2015; 108: 518–525.
 30. Scalici T, Fiore V and Valenza A. Experimental assessment of the shield-to-salt-fog properties of basalt and glass fiber reinforced composites in cork core sandwich panels applications. *Compos B Eng* 2018; 144: 29–36.
 31. Shi J, Wang X, Wu Z, et al. Fatigue behavior of basalt fiber-reinforced polymer tendons under a marine environment. *Construct Build Mater* 2017; 137: 46–54.
 32. Mousa S, Mohamed HM, Benmokrane B, et al. Flexural behavior of full-scale circular concrete members reinforced with basalt FRP bars and spirals: Tests and theoretical studies. *Compos Struct* 2018; 203: 217–232.
 33. Zhang X, Gu X and Lv J. Effect of basalt fiber distribution on the flexural-tensile rheological performance of asphalt mortar. *Construct Build Mater* 2018; 179: 307–314.
 34. Zhang X, Gu X, Lv J, et al. Mechanism and behaviour of fiber-reinforced asphalt mastic at high temperature. *Int J Pavement Eng* 2018; 19: 407–415.
 35. Alves SMC, Da Silva FS, Donadon MV, et al. Process and characterization of reclaimed carbon fiber composites by pyrolysis and oxidation, assisted by thermal plasma to avoid pollutants emissions. *J Comp Mater* 2018; 52: 1379–1398.
 36. Burn DT, Johnson M, Warrior NA, et al. The usability of recycled carbon fibres in short fibre thermoplastics: interfacial properties. *J Mater Sci* 2016; 51: 7699–7715.
 37. Liu Y, Farnsworth M and Tiwari A. A review of optimisation techniques used in the composite recycling area: State-of-the-art and steps towards a research agenda. *J Cleaner Production* 2017; 140: 1775–1781.
 38. Miracle DB and Donaldson SL (eds) *Glass fibers. ASM Handbook, Vol. 21: Composites*. Materials Park, OH: ASM International, 2001, pp.27–34.
 39. Kolesov YI, Kudryavtsev MY and Mikhailenko NY. Types and compositions of glass for production of continuous glass fiber (review). *Glass Ceram* 2001; 58: 197–202.
 40. Vas LM, Pölöskei K, Felhs D, et al. Theoretical and experimental study of the effect of fiber heads on the mechanical properties of non-continuous basalt fiber reinforced composites. *Express Polym Lett* 2007; 1: 109–121.
 41. Czigány T, Vad J and Pölöskei K. Basalt fiber as a reinforcement of polymer composites. *Periodica Polytech Ser Mech Eng* 2005; 49: 3–14.
 42. Chen K, Zhou N, Liu B, et al. Improved mechanical properties and structure of polypropylene pipe prepared under vibration force field. *J Appl Polym Sci* 2009; 114: 3612–3620.
 43. Yang L and Thomason JL. Effect of silane coupling agent on mechanical performance of glass fibre. *J Mater Sci* 2013; 48: 1947–1954.
 44. Thomason JL. The influence of fibre properties of the performance of glass-fibre-reinforced polyamide 6.6. *Compos Sci Technol* 1999; 59: 2315–2328.
 45. Deák T and Czigány T. Chemical composition and mechanical properties of basalt and glass fibers: A comparison. *Textile Res J* 2009; 79: 645–651.
 46. Hitchon JW and Phillips DC. The dependence of the strength of carbon fibres on length. *Fibre Sci Technol* 1979; 12: 217–233.
 47. Pardini LC and Manhani LGB. Influence of the testing gage length on the strength, Young’s modulus and Weibull modulus of carbon fibres and glass fibre. *Mater Res* 2002; 5: 411–420.
 48. MacFarland TW. *Two-way analysis of variance*. New York: Springer, 2011.
 49. Lim T and Loh W. A comparison of tests of equality of variances. *Comput Stat Data Anal* 1996; 22: 287–301.
 50. Nakamura AM, Michel P and Setoh M. Weibull parameters of Yakuno basalt targets used in documented high-velocity impact experiments. *J Geophys Res* 2007; 112. DOI: 10.1029/2006JE002757.
 51. Weibull W. A statistical distribution function of wide applicability. *J Appl Mech* 1951; 18: 293–297.
 52. Thomason JL. On the application of Weibull analysis to experimentally determined single fibre strength distributions. *Compos Sci Technol* 2013; 77: 74–80.
 53. da Costa LL, Loiola RL and Monteiro SN. Diameter dependence of tensile strength by Weibull analysis: Part I. Bamboo fiber. *Materia (Rio J)* 2010; 15: 110–116.
 54. Bevitori AB, Da Silva ILA, Lopes FPD, et al. Diameter dependence of tensile strength by Weibull analysis: Part II. Jute fiber. *Materia (Rio J)* 2010; 15: 117–123.
 55. Summerscales J, Hall W and Virk AS. A fibre diameter distribution factor (FDDF) for natural fibre composites. *J Mater Sci* 2011; 46: 5876–5880.
 56. Lee SM (ed.) *Handbook of composite reinforcements*. New York: Wiley, 1992.
 57. Otto WH. Relationship of tensile strength of glass fiber to diameter. *J Am Ceram Soc* 2006; 38: 122–125.
 58. Jung T and Subramanian RV. Strengthening of basalt fiber by alumina addition. *Scripta Metallurgica Materialia* 1993; 28: 527–532.